JETIR.ORG ISSN: 2349-5162 | ESTD Year : 2014 | Monthly Issue
JOURNAL OF EMERGING TECHNOLOGIES AND INNOVATIVE RESEARCH (JETIR)
An International Scholarly Open Access, Peer-reviewed, Refereed Journal

Groundwater hydrogeochemistry from the Command Area of the River Mutha and Bhima basin, Maharashtra, India.

[1]Dr. Kiran Sharad Kumbhar, [2]Mayur Shinde

[1] Assistant Professor, [2] Research Scholar
[1]Department of Geology,
[1]Nowrosjee Wadia College, Pune, India

Abstract: This study aimed to evaluate the hydrogeochemical properties of groundwater collected from the mutha river cross-section. To achieve this, 30 groundwater samples were collected and analyzed for various parameters, including pH, electrical conductivity, total dissolved solids, and ions such as sodium, potassium, calcium, magnesium, chloride, sulfate, nitrate, carbonate, hydrogen carbonate, and fluoride. The water quality was determined using the water quality index and Wilcox diagram. The fluid properties, irrigation water characteristics, and ion balance were analyzed using the Piper diagram to classify the type of water. The results showed that the water quality index for eleven samples from the right bank and eight samples from the right bank was excellent quality water (63.33%).

In comparison, three samples from the left bank and seven samples from the left bank were classified as good water (26.77%) based on the Wilcox diagram. The overall quality of the groundwater is considered excellent, reasonable, and permissible. The hydrochemical facies on the right bank was a calcium-chloride type, while on the left was a magnesium-hydrogen carbonate type.

Key Words: Groundwater Hydrogeochemistry, Total Dissolved Solids, Deccan Plateau

1. Introduction

Groundwater quality and its geochemical attributes are often influenced by both natural and human activities (Zhaoshi et al., 2021). The rapid development of agriculture and industry, as well as urbanization, is putting a significant strain on groundwater resources and leading to environmental changes that threaten long-term sustainability (Dhawan, 2017; Arulbalaji et al., 2019). Rivers provide essential water resources for irrigation, industry, and domestic use, and both natural and human activities can affect the hydrogeochemical characteristics and quality of groundwater in river basins (Panaskar et al., 2016). Both natural and human-induced actions often influence the characteristics of groundwater and its geochemical attributes. The increasing pace of agriculture and industrial development, as well as urbanization, is putting a significant strain on groundwater resources and leading to adverse environmental changes that may threaten long-term sustainability. Rivers provide essential water resources for irrigation, industry, and domestic purposes but can also be affected by natural and human-induced activities. These impacts on surface waters can lead to long-term changes in surface and subsurface water quality due to the release of pollutants from industries, urban areas, and agricultural areas.

Groundwater and surface water are interconnected through bidirectional fluxes that affect their physical, chemical, and biological conditions. Among the most famous volcanic regions on Earth is the Deccan Volcanic Province (DVP) of the Cretaceous-Eocene age (Krishnan 1982), where there is an imprint of erosion on the continents left by rivers in the form of dissolved and particulate materials. Traditionally, it has been characterized by monsoon settings with moderate rains (2,000–3,000 mm) in coastal lowlands and high rainfall in the Western Ghats (4,000–6,000 mm) that merges with the rainshadow zone of the Upland Plateau (Pawar and Kale, 2006). Most of the solutes in rivers are derived from the chemical weathering of minerals found in the rocks of the drainage basin. As a result of chemical weathering, rocks consume CO2, a greenhouse gas that substantially impacts climate (Berner et al., 1983; Kump et al., 2000; Amiotte-Suchet et al., 2003; Dessert et al., 2003).

Several parameters influence the rate and intensity of chemical weathering and associated carbon dioxide emissions. Recent research on basaltic provinces suggests they weather more rapidly because their lithologies, such as Granites and gneisses, exert a significant influence on marine geochemical balances and global change (Meybeck, 1986; Bluth and Kump, 1994; Amiotte-Suchet and Probst, 1995; Louvat and Allegre, 1997; Dessert et al., 2001; Amiotte-Suchet et al., 2003; Dessert et al., 2003).

As a result, the province has been premeditated from the point of view of chemostratigraphy (Beane et al. 1986; Mitchell and Widdowson 1991; Subbarao et al. 1988, 1994), petrology (Sen 1986), mineralogy and geochemistry (Sethna et al. 1996; Melluso et al. 1999), as well as geochronology and paleomagnetism (Prasad et al. 1996; Subbarao et al. 1988). Quantitative criteria have primarily governed the hydrogeological system of this hard rock terrain because the area comes under a semi-arid climatic zone.

The flow of groundwater from recharge to discharge areas has been delineated by a range of hydrogeochemical processes (Lakshmanan et al. 2003), but divergence in geochemistry can also result from hydro-geomorphological, hydrogeological, and anthropogenic factors (Drever 1982; Stuyfzand 1999; Rabemanana et al. 2005; Van der Weijden and Pacheco 2006; Traits et al. 2006). It is expected that a system restricted in set-up, such as a watershed with uniform lithology, the least amount of climatic variability, and no urbanization and industrialization, will offer a chance to identify lithogenic factors. Groundwater, on the other hand, is in prolonged contact with rocks, allowing it to interact with minerals, which are otherwise apathetic sufficiently. During this study, the main objectives were (1) to evaluate factors that govern the chemical composition of groundwater in fractured/weathered basaltic aquifers, (2) to evaluate dissolved solute inputs from different mineral reactants and determine the geochemical processes, and (3) evaluate mechanisms of weathering of basalts, chemical denudation rates, and insinuation into basalts on carbon dioxide absorption.

2.1 Type Style and Fonts

The study area is located approximately 180 km east of Mumbai in the Pune district of the Deccan Trap Province of India. Eventually, the Mutha meets the Bhima and Krishna rivers before draining into the Bay of Bengal. At the headwater of the basin, which covers an area of about 250 km2, industrialization and urbanization abound, with a few maximum patches of agriculture. The watershed reviewed as part of this study is in the rainshadow zone of the Western Ghats region or Sahyadri Mountain ranges, with annual rainfall ranging from 500 to 862 mm (average 750 mm/yr). Since the average precipitation has been nearly constant for over a decade, excess rain has occurred. These conditions have given rise to a semi-arid climate along the investigated geographic transect. Previous hydrogeological and geomorphological studies in and around the present area have been conducted by Rajaguru et al. (1993); Bondre et al. (2006); Aher et al. (2012); Joshi et al. (2013); Deshmukh et al. (2017) and Aher and Deshmukh (2019). The agricultural land is mainly scattered along waterways with various crops, while the mountainous and hilly areas are under degraded forests beside grasslands on hill slopes and rolling plains.

The selected cross-section is geologically and geomorphologically distinct, with one end connected with the Mutha basin in the south and the other to the Bhima basin in the north. The Mutha flows from west to east, and the samples collected from the cross section are equidistant from the right (south) and left (north) banks of the River (Table 1). The streams and tributaries in the region have their origins in nearby hilly areas and join the Mutha river at various locations. Geomorphologically, the site is composed of a mix of dissected hills, plateaus, and plains drained by the Mutha and Bhima Rivers tributaries. This River, an essential source of drinking water and irrigation in Maharashtra, India, flows through an area near the Pune district (Fig. 1). It is a seasonal river that relies on monsoonal precipitation and is a significant source of groundwater recharge. In this area, alternating bands of compact, amygdaloidal basalt flows and physically and chemically weathered rocks of Deccan traps.

The thickness of the classic compound pahoehoe rocks ranges from a few feet to 50 meters, made up of distinct flow sections ranging from a few centimeters to around 20 meters (Bondre et al., 2004; Aher et al., 2014). In the middle part of the region, there are colluvial-alluvial deposits around 30 meters thick, which are part of the late Quaternary Pravara formation (Bondre, 1999). The general framework of the formations from which the samples were collected. The depth refers to the groundwater from which the water samples were collected from wells. Abundant groundwater zones can generally be found within the DVP due to weathered, jointed, zeolitic, and vesicular traps (Prabhakaran, 1984).

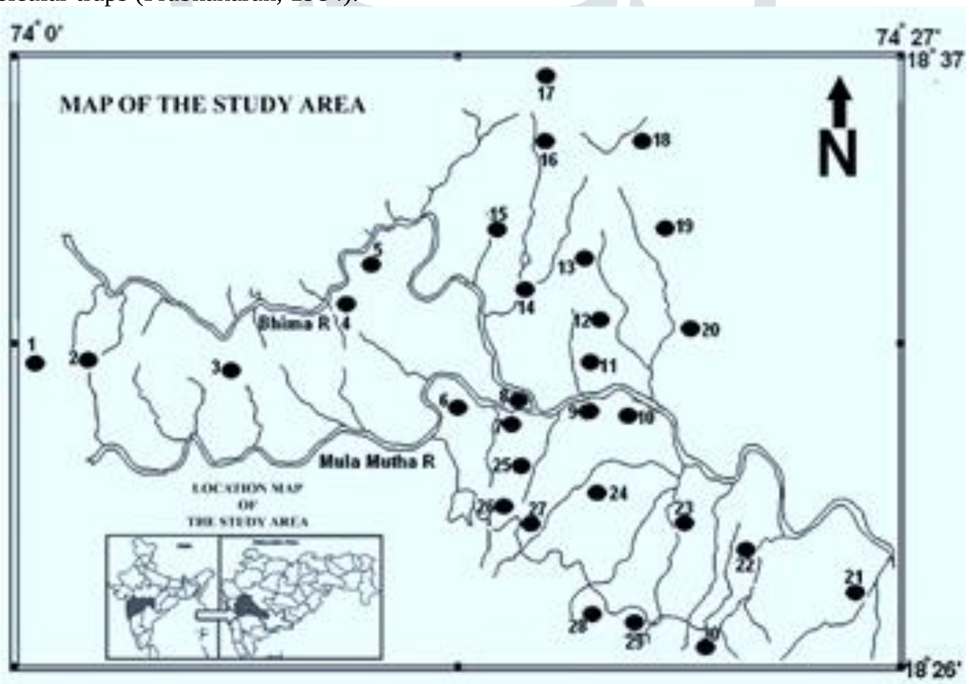

Fig. 1 Location map of the study area

2.2 Geological and Petrological Characteristics

DVP is one of the world's most important Large Igneous Provinces (LIP), which records a massive accumulation of tholeiitic magmas within a relatively short time period at the KePg boundary (e.g., Chenet et al., 2007, 2008, 2009). Several fissures caused lavas to flow out and drop down in lacustrine or terrestrial environments (Nair and Bhusari, 2001).

The study area distinguished by basalts of DVP that encompass an emaciated tuffaceous layer referred to as red boles. Compound lava flows from the region of Main Deccan Plateau Formation (Omkar Verma and Ashu Khosla 2019). This flows shows fine grade baslat where geochemical analysis revels that central part od pune from where river Mutha flows and meets to bhima are enriched with Na+ and k+ and the downstream portion from of River Bhima shows gradual enrichment of Ca++. also there ia comparitive enrichment of Fe++ and Fe+3 are seen in porphyritic flows. Phenocryst of Ca++ feldspar found in down south side of River bhima.

Trace element like Ni, Pb, Cr, Sr, and V are found in abundant in amount in central portion of pune while the amount of this trace element get decreases in down south oif River Bhima. Relative depletion of Ni, Zr and Pb found near the confluence of River Mutha and Bhima (Kanegaonkar, N., 1977)

2.3 HYDROGEOLOGICAL SETTINGS

The Deccan basalts, one of the world's largest volcanic provinces, are located in western India. They cover an area of 5105 km2, with a volume of 106 km3. (Courtillot et al., 1986). Lithospheric characteristics of the drainage basins of the Mutha, Bhima, and the other rivers sampled are predominantly tholeiitic basalts. In some of these tholeiites, forsterite has been found between Fo77 and Fo88 (Sen, 1980; Sen, 1986; Beane, 1988), and plagioclase phenocrysts have been found (Sen, 1980; Sen, 1986; Beane, 1988). Despite having relatively little porosity or permeability, the massive rocks function as an unyielding zone; however, due to joints, fracturing, and weathering, moderately porosity-containing structures are occasionally formed (Naik et al. 2003). While cavities, vesicles, flow contacts, lava tunnels, and pipes can build up porosity in the basalt (Pawar and Shaikh 1995), the flows in the study area are relatively impermeable. Bhargava and Bhattacharjee (1982) describe black soils as fine-textured with abundant smectite. Several of these soils are salt-affected, containing chlorides, bicarbonates, and carbonates of sodium in different proportions.

3 Materials and Methodology

3.1 Sampling and physico-chemical analysis

The Muha and Bhima basin shows relatively less diversity in terms of its geological, hydrological, climatic, and environmental characteristics than large river basins. Thus, the geochemical eccentricity of groundwater can be attributed to the imprint of mineralogical and chemical constituents of basaltic flows. Based on these considerations, 30 sampling sites in Post and Pre- Monsoon were selected for groundwater monitoring to represent lithology, aquifers, slope conditions, and land use. These samples represent 21 dug wells and 8 bore wells one surface water sample that wrap alluvial, basaltic, and dyke aquifers. Plastic containers with a capacity of about 1 ltr. were used for collecting water samples. The well was pumped for half an hour before groundwater samples were collected. When hand pumps were used to pump bore wells, samples were collected after hand pumping the bore well for a few minutes. Surface water samples were taken from flowing streams. Aquifer type, pH, E.C., well depth, static water level, and lithologies were also measured in the field. There were 90 samples collected to determine the seasonal trends in groundwater geochemistry.

Anons and cations were analyzed using a Dionex-Dx-600 High-Performance Ion Chromatography System. Anions were detected using AS-II-HC, a 4mm column, potassium hydroxide as eluent 'A'; and sodium hydroxide as eluent 'B.' A flow rate of 1.0 ml/min, an injection volume of 10 L.L., and a temperature of 30 C were used in the analysis ASRS-ULTRA, auto suppression external water mode, range 200 lS with suppressed conductivity. The cations (Na, K, Mg, and Ca) were analyzed using CS-12A analytical column. The flow rate of 1.0 µ/min was maintained by injecting a 25 µl sample and using sulfuric acid as eluent to pass the sample through a self-regenerating cation suppressor at room temperature. The concentrations of F, Cl, NO3, PO43-, SO4-2, Na, K, Mg, and Ca were determined using this method.

Table 1 Physico-chemical analysis of groundwater samples for the Pre-monsoon (April 2021)

Sr. No.	Location	pH	EC	TDS	Hardness	Ca	Mg	Na	K	Si	SiO2	F	Cl	HCO3-	CO2	SO4-2	NO3-	PO43-	Fe
1	W1	8.57	721	432.6	320	40.08	53.6	75	30	127	12.7	0.8	122	310	35.2	14	5.29	0.153	52
2	W2	8.99	736	441.6	268	41.68	40	63	9	161	16.1	1.2	116	270	13.2	17	26.4	0.323	103
3	W3	8.74	996	597.6	372	60.92	53.6	90	13	219	21.9	1.5	187	290	6.6	30	22.3	0.675	175
4	W4	8.4	1940	1164	688	79.78	83.1	315	27	153	15.3	1.9	315	450	30.8	170	16.8	0.148	456
5	W5	8.63	1520	912	604	139.5	62.4	102	23	162	16.2	2.5	233	310	15.4	115	24.6	0.221	528
6	W6	8.26	1040	624	364	320.6	106	90	28	169	16.9	2.4	156	340	44	35	17.1	0.234	502
7	W7	8.6	1340	804	428	59.32	68.2	160	9	154	15.4	2.1	207	370	22	54	14.5	0.109	631
8	W8	8.71	1540	924	276	52.11	33.1	193	44	191	19.1	2.3	193	530	19.8	51	14.1	0.211	709
9	BW 1	8.78	1980	1188	772	70.54	145	300	13	190	19	2.7	338	380	28.6	150	25.2	0.056	589
10	BW 2	8.31	1960	1176	704	110.6	104	287	18	176	17.6	2.9	301	420	52.8	160	71.2	0.393	710
11	W 9	8.4	987	592.2	536	105.8	66.3	243	18	183	18.3	2.4	261	290	22	135	11.9	0.691	859
12	BW 3	8.81	1630	978	420	99.4	41.9	150	9	192	19.2	2.1	264	180	8.8	110	9.3	0.701	547
13	BW 4	8.44	870	522	340	78.56	35.1	54	34	183	18.3	1.9	215	250	19.8	15	45.3	0.43	410
14	W 10	8.33	2480	1488	544	81.38	77	440	37	176	17.6	2.2	471	580	39.6	130	30.9	0.008	610
15	BW 5	8.4	614	368.4	272	57.72	31.2	32	14	165	16.5	2.1	85.2	270	8.8	10	16.8	0	652
16	BW 6	8.68	449	269.4	204	32.06	30.2	28	9	212	21.2	1.7	90.9	200	13.2	7	5.9	0.396	210
17	W 11	8.62	823	493.8	380	75.35	46.8	43	29	208	20.8	1.5	168	300	30.8	15	24.9	0.359	115
18	W 12	8.56	1030	618	464	59.32	77	52	8	199	19.9	1.9	204	280	19.8	29	16.3	0.069	649
19	W 13	8.55	767	460.2	268	35.27	43.9	70	6	220	22	2	125	370	19.8	18	11.9	0.007	692
20	BW 7	8.49	1480	888	672	125	87.7	65	33	208	20.8	2.3	329	250	15.4	43	51.2	0	843
21	BW 8	8.69	2100	1260	404	20.84	85.8	380	11	179	17.9	2.4	432	630	26.4	35	3.9	0	1202
22	W 14	8.88	600	360	256	36.87	40	39	7	171	17.1	2.2	119	200	17.6	11	10.3	0.114	954
23	W 15	8.35	1540	924	660	97.8	101	105	23	166	16.6	2.1	239	390	41.8	125	11.4	0.099	873
24	W 16	8.5	808	484.8	388	36.87	72.1	52	7	191	19.1	1.8	105	360	26.4	12	22.8	0.072	824

25	W 17	8.49	866	519.6	404	40.08	74.1	47	5	180	18	1	211	310	16.28	28	34.1	0.115	789
26	W 18	8.68	1650	990	480	73.75	72.1	230	43	189	18.9	1.9	344	380	19.8	46	85.2	0.053	429
27	W 19	8.47	677	406.2	308	33.67	54.6	39	2	210	21	1.6	105	270	17.6	10	44.9	0.037	382
28	R	8.78	308	184.8	144	30.46	16.6	15	13	201	20.1	1.4	85.2	140	6.6	7	0	0	438
29	W 20	8.36	1310	786	452	56.11	76	89	11	182	18.2	1.1	239	450	35.2	21	23.1	0.136	470
30	W 21	8.53	734	440.4	296	35.27	50.7	77	52	201	20.1	1.2	114	350	17.6	5	0	0	506

Table 2 Physico-chemical analysis of groundwater samples for the Pre-monsoon (April 2021)

Sr. No.	Location	pH	EC	TDS	Hardness	Ca	Mg	Na	K	Si	SiO_2	F	Cl	HCO_3^-	CO_2	SO_4^{-2}	NO_3-	PO_4^{3-}	Fe
1	W1	8.02	610	366	320	74.17	110	56.8	0.8	52	5.2	1.1	213	450	30.8	30	13.3	0.301	65
2	W2	7.7	740	444	240	112.2	97.5	68	0.8	106	10.6	1.5	56.8	550	35.2	63	51.8	0.653	124
3	W3	7.89	1040	624	290	92.6	79.2	91.4	0.7	103	10.3	1.4	121	350	30.8	112	41.2	1.323	252
4	W4	7.63	1860	1116	395	108.2	170	158	1.3	53.7	5.37	2.2	185	450	44	450	29	0.269	663
5	W5	7.92	1550	930	395	132.3	124	103	1.8	59.5	5.95	2.1	199	350	17.6	300	46.5	0.525	762
6	W6	7.4	1040	624	250	90.2	82.6	92.4	1.5	84.5	8.45	2.6	99.4	400	48.4	122	32.8	0.525	722
7	W7	7.42	1480	888	330	88.18	114	127	0.8	82.8	8.28	2.5	128	500	22	298	28.8	0.206	910
8	W8	7.65	1490	894	240	82.18	90.3	163	3.3	51.4	5.14	2.2	85.2	750	22	11	27	0.525	1021
9	BW 1	7.84	2130	1278	405	92.18	162	152	1	108	10.8	2.9	241	500	13.2	386	51.4	0.11	848
10	BW 2	7.54	2540	1524	465	125.3	171	161	2.8	50.3	5.03	2.6	263	500	44	418	143	0.716	1035
11	W 9	7.68	2345	1407	350	124.2	190	157	1.9	110	11	2.5	475	310	35.2	565	24.6	1.323	1237
12	BW 3	8.07	2030	1218	295	108.2	156	151	1.6	105	10.5	2.3	334	200	13.2	346	19.3	1.483	789
13	BW 4	7.7	1120	672	300	104.2	166	64.1	2.4	61.3	6.13	2	142	300	13.2	344	89.7	0.94	590
14	W 10	7.95	1630	978	330	104.2	120	205	2.3	86.9	8.69	2.4	195	700	33	172	61.1	0.014	878
15	BW 5	7.5	650	390	240	88.18	127	45.3	0.7	110	11	2.2	142	600	13.2	15	34.6	0	937
16	BW 6	7.48	490	294	200	36.2	40.6	35.8	0.2	122	12.2	1.8	65.3	200	17.6	21.3	12.4	0.812	302
17	W 11	7.34	740	444	255	51.3	59.8	43.3	0.7	107	10.7	1.9	8.52	400	30.8	16	50.1	0.685	166
18	W 12	7.39	1220	732	375	81.19	98.5	71.4	0.5	87.4	8.74	1.7	34.1	550	26.4	96	31.5	0.142	935
19	W 13	7.83	800	480	235	51.3	68.4	77.7	0.9	122	12.2	2.3	8.52	500	26.4	38.5	21.3	0.014	1053
20	BW 7	7.51	1320	792	375	75.3	97.6	67.5	1.7	108	10.8	2.7	34.1	400	17.6	152	101	0	1214
21	BW 8	7.92	1120	672	225	34.15	52.1	128	1.2	155	15.5	2.6	30.5	500	11	55	7.53	0	1731
22	W 14	8.14	530	318	200	40	56.1	39.9	0.6	122	12.2	2.5	10.2	375	11	5.5	19.7	0.238	1374
23	W 15	7.43	8540	5124	250	72.14	156	58	3	121	12.1	2.3	309	550	30.8	241	20.8	0.206	1257
24	W 16	7.91	1160	696	290	32.14	54.1	73.2	0.5	154	15.4	2.1	18.9	500	13.2	3.5	47	0.142	1187
25	W 17	7.37	3260	1956	530	42.18	74	210	1.4	143	14.3	0.9	85.2	640	33	20	66.9	0.238	1134
26	W 18	7.55	2200	1320	385	40.16	67.8	172	4.7	119	11.9	1.7	64	550	35.2	9	173	0.11	617
27	W 19	7.55	1060	636	775	72.18	94.2	65.6	0.3	133	13.3	1.5	17	550	26.4	31	87.5	0.078	551
28	R	7.86	370	222	175	42.18	38.5	14.6	0.6	125	12.5	1.7	7.1	350	8.8	9.5	traces	0	631
29	W 20	7.42	1140	684	340	41.16	43.9	81.8	0.6	142	14.2	1.3	25.5	580	6.6	14	45.2	0.269	677
30	W 21	7.49	760	456	220	34.17	41.1	70.3	2.6	131	13.1	1.4	14.2	400	4.4	20	traces	0	730

4. Results and Discussion

Table no. 1 and 2 gives the pH, temperature, E.C., and significant ion concentrations of river waters analyzed for the pre and post-mosoon seasons. In general, the pH of the samples varies from close to neutral to mildly alkaline, ranging from for pre-monsoon is in between 7.26 to 8.99, with most within the range of 7.34 to 8.14 observed for post-monsoon season. The highest concentrations of alkalinity are found in the Bhima river. The samples range from 308 to 8540 µ*S*cm^{-1} in terms of their E.C. Samples collected near river origins have lower values because of dilution resulting from heavy rainfall. The temperature ranges between 22 and 30 °C. About 70% of the total anions in the groundwater are HCO3 (Tables 1 and 2), with values ranging from 200 to 750 mg/l (avg. 465.167 mg/l).

By interpreting hydrochemical diagrams along with distribution maps and hydrochemical sections, hydrogeochemical charts can be used to analyze evolution trends, especially in groundwater systems. About 19.78% of the total anions in the groundwater are HCO_3^- (Tables 2 and 3), with minimum values ranging from 112 to 200 mg/l (avg. 140 mg/l) and maximum values ranging from 300 to 630 mg/l (avg. 456 mg/l). The samples from dug wells near the source of the Mutha River have a lower Cl content than SO_4 (Table1 and 2), with an equivalent Cl/SO_4 ratio of 0.39. HCO_3^- shows an overall increasing trend for silica. Silica shows a general increasing trend with HCO_3^-. The total dissolved solids (TDS) in the waters (Table 1) vary over a wide range, 184 to 1488 mg l^{-1} and 222 to 5124 mg l^{-1}, with a mean for Pre-monsoon is 709 mg $l^{-1,}$ and for Post monsoon, it is 939 mg l^{-1}

4.1 Water quality index

The Water Quality Index (WQI) is a commonly used method for evaluating the quality of groundwater for drinking purposes in various parts of the world. In this study, the WQI was used to determine the quality of the water in the sampled area as being either poor, good, or excellent. The water was found to have excellent quality due to the lack of any significant hazards. The WQI model proposed by Vasanthavigar et al. (2010) and Ravikumar et al. (2013) was used in this study, which involves assigning weights to different chemical parameters based on their importance in determining the overall water quality and creating a score scale. Poor quality water is prone to natural fluctuations that can cause it to deviate from natural or desired levels (Neary et al., 2001). The quality of the water was determined using a comparative weighted method (Wang et al., 2017), which takes into account various parameters such as those described by Horton (1965), Tiwari et al. (2014, 2017).

The importance of 11 chemical parameters in the overall quality of drinking water was assessed by assigning weights to each of them (Table 3). The parameters with the greatest impact on water quality, TDS, fluoride, chloride, nitrate, sulphate, and sodium. Bicarbonate, however, was found to have a minimal impact on water quality according to Singh and Hussian (2016). Therefore, the calculated value for water quality index is 27.33 which is fits into the Good quality of water. (by the eq. 1)

$$\mathbf{WQI} = \Sigma W_i Q_i \qquad \text{.................(eq.1)}$$

Where, W_i= Unit weightage and Q_i= Sub index of i^{th} parameter.

Table 3 Chart of experimental parameters and comparisons with standards.

Parameters		Range	Avarage (Vi)	Relative weight (Wi)	Sub index Parameter (Qi)	WHO (1997) Max. Desirable (Si)	WHO (1997) Max. Desirable	BIS (2003) IS (10500) Max. Permissible	BIS (2003) IS (10500) Max. Permissible
General	pH	7.34-8.14	7.67	9E-04	0.902352941	7.0-8.5	6.5-9.2	6.5-8.5	8.5-9.2
	EC (µS/cm)	370-8540	1565.5	-		-	-	-	-
	TDS (mg/L)	222-5124	939.3	1E-05	1.8786	500	1500	500	2000
Major Cations	Ca^{2+} (mg/L)	32.14-132.3	75.7413	1E-04	1.009884444	75	200	75	200
	Mg^{2+} (mg/L)	38.5-190	100.077	2E-04	3.335888889	30	150	30	100
	Na^+ (mg/L)	14.6-21	100.137	1E-04	2.002733333	50	200	-	-
	K^+ (mg/L)	0.2-4.7	1.44	7E-05	0.0144	100	200	-	-
	Cl^- (mg/L)	7.1-475	120.385	3E-05	0.481538667	250	600	250	1000
Major Anions	HCO_3^- (mg/L)	200-750	465.167	4E-05	2.325833333	200	600	200	600
	SO_4^{-2} (mg/L)	3.5-565	145.477	-	0.727383333	200	600	200	400
	NO_3^{2-} (mg/L)	7.53-173	49.2154	-	13.30456494	-	50	45	100
	F^- (mg/L)	0.9-2.9	2.03	0.005	1.353333333	0.6-1.5	1.5	1	1.5

4.2 Wilcox plot

The Wilcox diagram, developed by Wilcox in 1955, was used to classify water based on its sodium content and electrical conductivity. According to Wilcox (1948, 1955), water quality for irrigation purposes can be classified into five categories: excellent (sodium content < 20%), good (sodium content 20-40%), permissible (sodium content 40-60%), doubtful (sodium content 60-80%), and unsuitable (sodium content > 80%). The Wilcox diagram combines sodium content and electrical conductivity within predetermined ranges to classify water as Class I (excellent to good), Class II (good to permissible), Class III (permissible to doubtful), Class IV (doubtful to unsuitable), or Class V (unsuitable) for irrigation purposes (Bhatti et al., 2019).

The Wilcox diagram (Fig 2and 3) shows that the majority of the groundwater in the study area is suitable for irrigation, with 64% falling into the good to permissible range and an additional 16% in the excellent to good range. Only 20% of the samples were in the permissible to doubtful range. These results indicate that the groundwater in the hilly tracks is particularly suitable for irrigation.

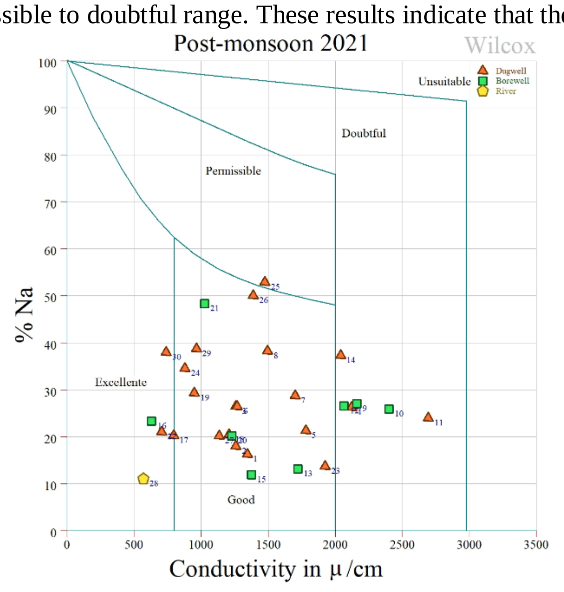

Fig. 2 Wilcox plot Post-monsoon 2021

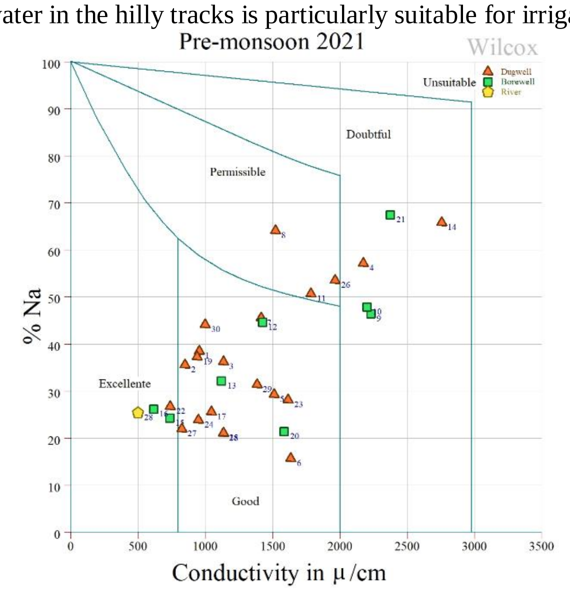

Fig. 3 Wilcox plot Pre-monsoon 2021

4.3 Irrigation water characteristics

The irrigation water quality of the analyzed groundwater samples was assessed using the Diagrammes software. This included evaluation of the exchangeable sodium ratio (ESR), sodium adsorption ratio (SAR), magnesium hazard, and salinity hazard based on Lloyd and Heathcote (1985). These measures help to determine the general suitability of the groundwater for agriculture. The SAR was calculated using the Diagrammes software and is a commonly used indicator for managing sodium-affected water and soil. The SAR was determined using the equation provided by the USDA (1954). The majority of slinity hazard class for study area was C3 which was around 70% for pre and Post-monsoon whereas class C2 was (20%) and class C4 was observed as 10% for post and Pre-monsoon. (Fig. 4 and 5). Also its depict from the fig. that alkalizing power for post monsoon was falls under class S1 whereas pre-monsoon lies on class S1 and S2.

$$SAR= \frac{[Na^{+}]}{\sqrt{\frac{[Ca^{2+}]+[Ma^{2+}]}{2}}} \quad \text{………………..(eq.2)}$$

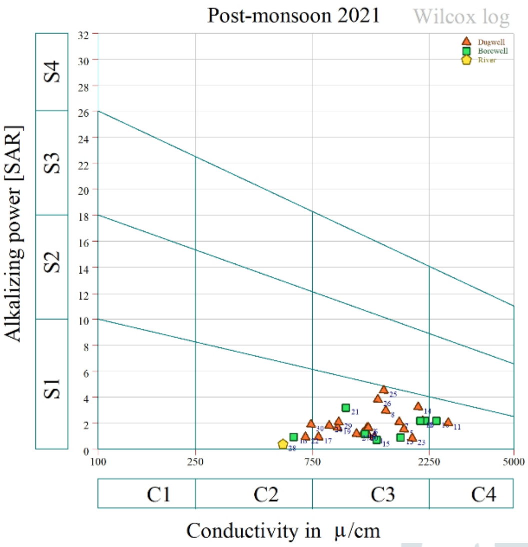

Fig. 4 SAR Post-monsoon 2021

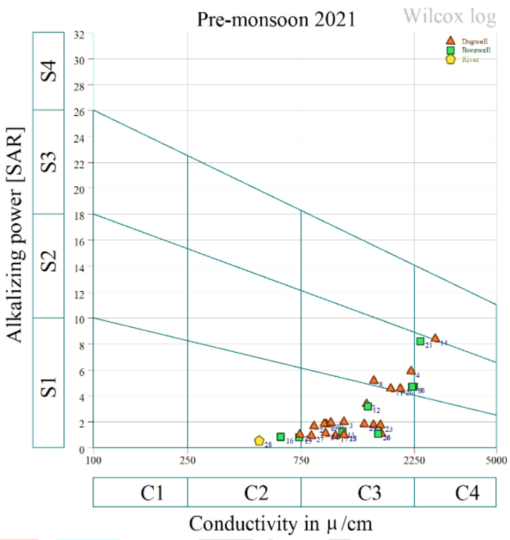

Fig. 5 SAR Pre-monsoon 2021

4.4 Piper diagrams

The physico-chemical analysis of the groundwater included the use of ion balance and Piper diagrams to understand the variations in the chemistry of the samples. The ion balance diagram was generated for samples from the right side and left side using the Diarammes software. This diagram displays the relative proportions of cations and anions in the water samples and their relation to their electrical equivalents (EE), which is a measure of the total charge of the ions present in the water based on their concentration and charge. Muhammad et al. (2004) explained that ion balance diagrams can provide insight into the composition of the water sample.

According to the Piper diagram, 20% of the samples belong to the Ca2+-Mg2+-HCO3- type, which is indicative of sufficient recharge and temporary hardness. Only 80% of the samples contain groundwater with permanent hardness, which is of the Ca2+-Mg2+-Cl-SO42- type. In terms of anion chemistry, 20% of the groundwater samples do not fall into any dominant zone, but the remaining 80% are of the bicarbonate and chloride type. The cation diagram shows that the majority (83.60%) of the groundwater samples fall into the Mg2+ zone, while 16.40% fall into the Na+ + K+ zone. No samples fall into the Ca2+ zone. Overall, the Piper trilinear diagram classifies the groundwater as primarily belonging to the hydrochemical facies of the Cl + SO4 >Ca + Mg type.

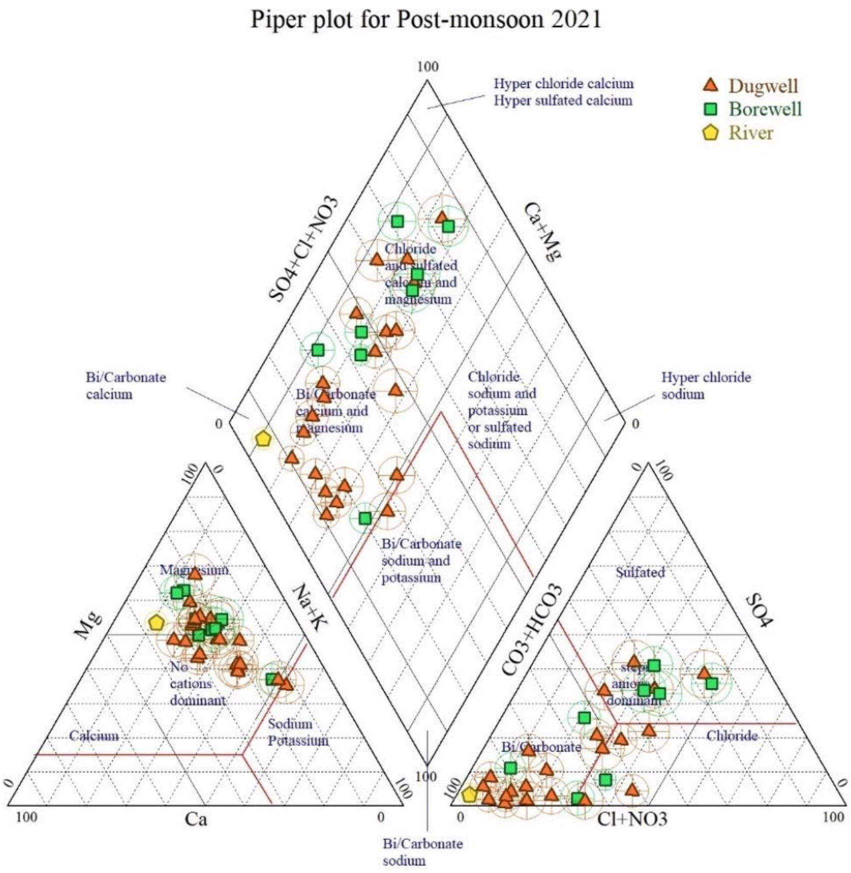

Fig. 6 Piper diagram in shallow groundwater for Post- Monsoon season

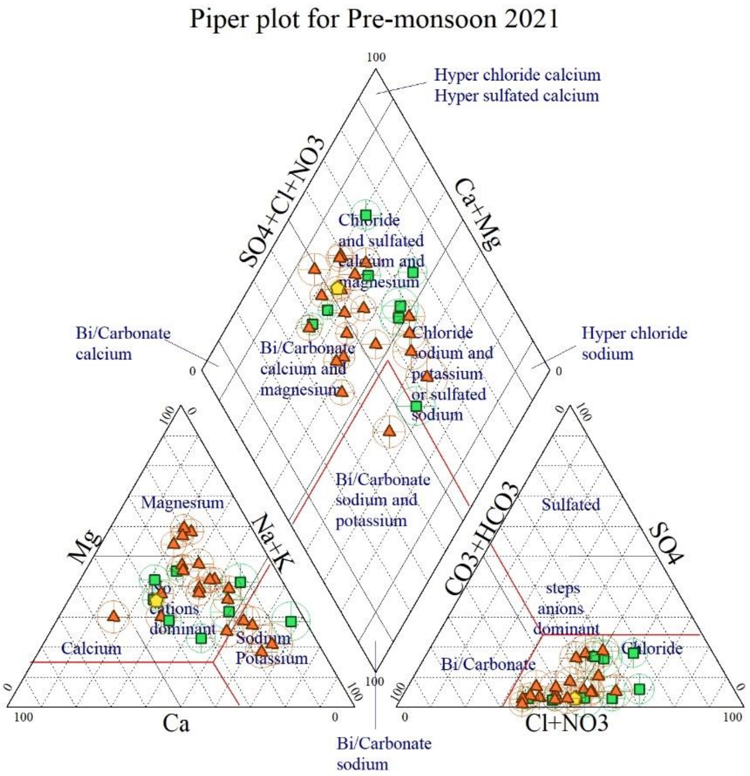

Fig. 7 Piper diagram in shallow groundwater for Pre- Monsoon season.

5. Conclusion:

A definite and precise geochemical investigation of the Command regions of the Mutha and the Bhima and various medium and little waterways draining the southwest Deccan Traps (India) has been done to decide the paces of chemical and silicate weathering of their basins and Deccan basalts overall. This study depends on recurrent examination of around two dozen streams north of two rainy seasons, 2020 and 2021.

1) TDS levels in the waters range from 184 to 1488 mg l^{-1} and 222 to 5124 mg l^{-1} (Fig. ___), with a mean for Pre-monsoon, is 709 mg $l^{-1,}$ and for Post monsoon, it is 939 mg l^{-1}; nevertheless, approximately half of the samples contain TDS levels of 600 mg l^{-1}. High Cl, SO4, and Na concentrations cause the high TDS levels in the Mutha and Bhima.

2) The most abundant cations and anions in the majority of rivers are (CaMg) and HCO3. Samples are calcite supersaturated, and several exhibit significant Cl, SO4, and TDS. Rivers with high Cl also have high SO4 levels; there is a significant association between the two and Na. If these data are interpreted in terms of supply from saline soils and anthropogenic sources, their average contribution to the Krishna and Bhima tributaries and the Mutha and Bhima mainstream would be 30 to 30 percent Cl and 60 to 64 percent Na, respectively.
3) According to the Water Quality Index (WQI), the groundwater quality was excellent within 64% of the samples, good in 16%, and poor in the remaining 20%.
4) The Piper diagram, 20% of the samples belong to the Ca2+-Mg2+-HCO3- type, which is indicative of sufficient recharge and temporary hardness. Only 80% of the samples contain groundwater with permanent hardness, which is of the Ca2+-Mg2+-Cl-SO42- type.

REFERENCES

[1] Aher, S.P., Shinde, S.D., Jarag, A.P., Mahesh, Babu, J., Gawali, P.B., 2014. Identification of lineaments in the Pravara basin from ASTER-DEM data and satellite images for their geotectonic implication. Int. J. Earth Sci. 2, 1–5.

[2] Aher, S.P., Bairagi, S.I., Deshmukh, P.P., Gaikwad, R.D., 2012. River change detection and bank erosion identification using topographical and remote sensing data. Int. J. Appl. Inf. Sys. 2, 1–7.

[3] Aher, S., Deshmukh, K., 2019. Identifying the impact of intensive agriculture practices on groundwater quality using GIS and multi-tracer techniques around Sangamner City. Geocarto Int. 36 (10), 1136–1160. https://doi.org/10.1080/ 10106049.2019.1633422.

[4] Amiotte-Suchet P. and Probst J. L. (1995) A global model for present day atmospheric/soil CO2 consumption by chemical erosion of continental rocks (GEN-CO2). Tellus 47B, pp. 273–280.

[5] Amiotte-Suchet P., Probst J. L., Ludwig W. (2003) Worldwide distribution of continental rock lithology: Implications for the atmospheric/soil CO2 uptake by continental weathering and alkalinity river transport to the oceans. Global Biogeochem. Cycles 17, pp. 1891–1903.

[6] Arulbalaji, P., Padmalal, D., Sreelash, K., 2019. GIS and AHP techniques Based Delineation of Groundwater potential Zones: a case study from southern Western Ghats, India. Sci. Rep. Nat. 9, 2082. https://doi.org/10.1038/s41598-019-38567-x.

[7] Beane J. E. (1988) Flow Stratigraphy, Chemical Variation and Petrogenesis of Deccan Flood Basalts, Western Ghats, India. Ph.D. Dissertation, Washington State University.

[8] Bean JE, Turner CA, Hooper PR, Subbarao KV, Walsh JN (1986) Stratigraphy, composition and form of Deccan Basalts, Western Ghats, India. Bull Volcano 48: pp. 61–83

[9] Berner R. A., Lasaga A. C., and Garrels R. M. (1983) The carbonate-silicate geochemical cycle and its effect on atmospheric carbon dioxide over the past 100 million years. Am. J. Sci. 284, pp.641–683.

[10] Bhargava G. P. and Bhattacharjee J. C. (1982) Morphology, genesis and classification of saltaffected soils. In Review of Soil Research in India, Part II, International Congress of Soil Sciences, Indian Society of Soil Science, New Delhi, pp. 508–528.

[11] Bhatti, E.-u.-H., Khan, M.M., Shah, S.A.R., Raza, S.S., Shoaib, M., Adnan, M., 2019. Dynamics of Water Quality: Impact Assessment Process for Water Resource Management. Processes 7 (2), 102. https://doi.org/10.3390/pr7020102.

[12] Bluth G. J. S. and Kump L. R. (1994) Lithologic and climatic control of river chemistry. Geochim. Cosmochim. Acta 58, pp. 2341–2359.

[13] Bondre, N.R., 1999. Geology of the area around Akole, Maharashtra (using remote sensing techniques). University of Pune. MSc thesis.

[14] Bondre, N.R., Duraiswami, R.A., Dole, G., 2004. Morphology and emplacement of flows from the Deccan Volcanic Province, India. Bull. Volcanol. 66 (1), 29–45.

[15] Bondre, N.R., Hart, W.K., Sheth, H.C., 2006. Geology and geochemistry of the Sangamner mafic dike swarm, western Deccan volcanic province, India: implications for regional stratigraphy. The J. of Geology. 114 (2), 155–170.

[16] Chenet, A.L., Courtillot, V., Fluteau, F., G erard, M., Quidelleur, M., Khadri, S.F.R., Subbarao, K.V., Thordarson, T., 2009. Determination of rapid Deccan eruptions across the CretaceouseTertiary boundary using paleomagnetic secular variation: 2. Constraints from analysis of eight new sections and synthesis for a 3500-m-thick composite section. J. Geophys. Res. 114, B06103.

[17] Chenet, A.L., Fluteau, F., Courtillot, V., Gerard, M., Subbarao, K.V., 2008. Determination of rapid Deccan eruptions across the CretaceouseTertiary boundary using paleomagnetic secular variation: results from a 1200-m-thick section in the Mahabaleshwar. J. Geophys. Res. 113, B04101.

[18] Chenet, A.L., Quidelleur, Z., Fluteau, F., Courtillot, V., Bajpai, S., 2007. 40Ke40Ar dating of the main Deccan large igneous province: further evidence of KTB age and short duration. Earth Planet. Sci. Lett. 263,

[19] Courtillot, V., Besse, J., Vandamme, D., Montigny, R., Jaeger, J.J., Cappetta, H., 1986. Deccan flood basalts at the Cretaceous/Tertiary boundary? Earth Planet. Sci. Lett. 80, 361e374.

[20] Deshmukh K. K, Aher S. P. (2017) Assessment of Soil Fertility Around Municipal Solid Waste Disposal Site Near Sangamner City, Maharashtra, India. Curr World Environ., 12(2), 401-410.

[21] Dessert C., Dupre B., Francois L. M., Schott J., Gaillardet J., Chakrapani G., and Bajpai S. (2001) Erosion of Deccan Traps determined by river geochemistry: impact on the global climate and the 87Sr/86Sr ratio of seawater. Earth Planet. Sci. Lett. 188, pp. 459–474.

[22] Dessert C., Dupre B., Gaillardet J., Francois L. M., and Allegre C. J. (2003) Basalt weathering laws and the impact of basalt weathering on the global carbon cycle. Chem. Geol. 20, pp. 1–17.

[23] Dhawan, V., 2017. Water and Agriculture in India. German Asia-Pacific Business Association, Imprint, pp. 1–25

[24] Drever J.I. (1982) The geochemistry of natural waters. Prentice Hall, New York, 182 pp.

[25] Horton, R.K., 1965. An index number system for rating water quality. J. Water Pollu. Cont. Fed. 37 (3), 300–305.

[26] Joshi, V.U., Daniels, M.J., Kale, V.S., 2013. Morphology and origin of valley-side Gullies formed along the watersheds of Deccan province, India, and rangeland of Colorado, USA. Transactions. 35 (1), 103–122.

[27] Kanegaonkar, N,. (1977), Geology of the Deccan Trap Country around Pune Maharashtra, Ph.D. Thesis, University of Poona.

[28] Krishnan MS (1982) Geology of India and Burma, 6th edn. CBS publishers and distributors, New Delhi.

[29] Kump L. R., Brantley S. L., and Arthur M. A. (2000) Chemical weathering, atmospheric CO2 and climate. Ann. Rev. Earth Planet. Sci. 28, pp. 611–667.

[30] Lakshmanan E, Kannan R, Senthil Kumar M (2003) Major ion chemistry and identification of hydrochemical processes of groundwater in a part of Kancheepuram district Tamilnadu, India. Environ Geosci 10(4): pp.157–166

[31] Lloyd, J.W., Heathcote, J.A., 1985. Natural inorganic hydrochemistry in relation to groundwater: an introduction. Clarendon, Oxford.

[32] Louvat P. and Allegre C. (1997) Present denudation rates on the island of Reunion determined by river geochemistry: Basalt weathering and mass budget between chemical and mechanical erosions. Geochim.Cosmochim. Acta 61, pp. 3645–3669.

[33] Melluso L, Sethna SF, Morra V, Khateeb A, Javeri P (1999) Petrology of mafic dyke swarm of the Tapti River in the Nandurbar area. In: Subbarao K.V. (ed) Deccan volcanic province, vol 3, no 1. Geol Soc India, Memoir, pp. 735–738

[34] Meybeck M. (1986) Composition chimique des ruisseaux non pollutes de France. Sci. Geol. Bull. (Strasbourg) 39, pp. 3–77.

[35] Mitchell C, Widdowson M (1991) A geological map of the Southern Deccan Trap, India and its structural implications. J Geol Soc London 148: pp.495–505

[36] Muhammad, N., 2004. Hydraulic, Diffusion, and Retention Characteristics of Inorganic Chemicals in Bentonite. A dissertation submitted to Department of Civil and Environmental Engineering College of Engineering. University of South Florida.

[37] Nair, K.K.K., Bhusari, B., 2001. Stratigraphy of Deccan traps: a review. Geol. Surv. India Spl. Publ. 64, 477e941.

[38] Naik PK, Awasthi AK (2003) Groundwater resources assessment of Koyna River basin, India. J Hydrol 11(5):82–594

[39] Neary, B., Cash, K., H´ebert, S., Khan, H., Saffran, K., Swain, L., Williamson, D., Wright., R., 2001. Canadian Water Quality Guidelines for the Protection of Aquatic Life. CCME Water Quality Index 1.0 Technical Report. Canadian Council of Ministers of the Environment. Winnipeg, Manit.

[40] Panaskar, D.B., Wagh, V.M., Muley, A.A., Mukate, S.V., Pawar, R.S., Aamalawar, M.L., 2016. Evaluating groundwater suitability for the domestic, irrigation, and industrial purposes in Nanded Tehsil, Maharashtra, India, using GIS and statistics. Arab. J. Geosci. 9, 615. https://doi.org/10.1007/s12517-016-2641-1.

[41] Pawar NJ, Shaikh IJ (1995) Nitrate pollution of groundwaters from shallow basaltic aquifers, Deccan Trap Hydrogeologic Province, India. Environ Geol 25:197–204

[42] Pawar NJ, Vishwas S Kale (2006) Waterfall tufa deposits from the Deccan Basalt Province, India: implications for weathering of basalts in the semi-arid tropics. Z Geomorph NF 145: pp.17–36

[43] Prasad JN, Patil SK, Saraf PD, Venkateshwarlu M, Rao DRK (1996) Palaeomagnetism of dyke swarms from the Deccan volcanic province of India. J Geomagn Geoelectr 48: pp.977–991

[44] Rabemanana V, Violette S, Marsily G de, Robain H, Deffontaines B, Andrieux P, Bensimon M, Parriaux A (2005) Origin of the high variability of water mineral content in the bedrock aquifers of Southern Madagascar. J Hydrol 310: pp.143–156.

[45] Rajaguru, S.N., Kale, V.S., Badam, G.L., 1993. Quaternary fluvial systems in upland Maharashtra. Quaternary Period in India. Curr. Sci. 64, 10–25.

[46] Ravikumar, P., Aneesul Mehmood, M., Somashekar, R.K., 2013. Water quality index to determine the surface water quality of Sankey tank and Mallathahalli lake, Bangalore urban district, Karnataka. India. Appl. Water Sci. 3 (1), 247–261.

[47] Sen G. (1980) Mineralogical variations in Delakhari Sill, Deccan Trap intrusion, Central India. Contrib. Mineral. Petrol. 75, 71–78.

[48] Sen G (1986) Mineralogy and petrogenesis of the Deccan trap lava flows around Mahabaleshwar, India. J Petrology 27: pp.627–663

[49] Sethna SF, Ateeq K, Javeri P (1996) Petrology of basic intrusives in the Deccan Volcanic Province south of Tapti Valley and their comparison with those along the west coast. Gond Geol Mag Spl Vol 2: pp.225–232.

[50] Stuyfzand PJ (1999) Patterns in groundwater chemistry resulting from groundwater flow. J Hydrogeol 7(1): pp.15–27.

Subbarao KV, Chandrasekharam D, Navaneethakrishanan P, Hooper PR (1994) Stratigraphy and structure of Parts of the central **[51]** Deccan Basalt Province: Eruptive Models, Volcanism, pp. 321–332.

Subbarao KV, Hooper PR (1988) Reconnaissance map of the Deccan basalt group in the Western Ghats, India. In: Subbarao K.V. (ed) Deccan flood basalts. Mem Geol Soc India, no. 10.

[52] Tarits C, Aquilina L, Ayraud V, Pauwel H, Davy P, Touchard F, Bour O (2006) Oxido-reduction sequence related to flux variations of groundwater from fractured basement aquifer (Ploemeur area, France). Appl Geochem 21: pp.29–47

[53] Twari, A.K., Singh, A.K., Mahato, M.K., 2017. Assessment of groundwater quality of Pratapgarh district in India for suitability of drinking purpose using water quality index (WQI) and GIS technique. Sustain. Water Resour. Manag. 4 (3), 601–616.

[54] Tiwari. A., Singh, P., Mahato, M., 2014. GIS-based evaluation of water quality index of groundwater resources in West Bokaro Coalfield. India. Curr. World Environ. 9 (3), 843–850.

[55] Usda, 1954. U.S. Salinity Laboratory Staff, Diagnosis and improvement of saline and alkali soils, handbook, No. 60. US Department of Agriculture, Washington.

[56] Van der Weijden CH, Pacheco FAL (2006) Hydrogeochemistry in the Vouga River basin (central Portugal): pollution and chemical weathering. Appl Geochem 21: pp.580–613.

[57] Vasanthavigar, M., Srinivasamoorthy, K., Vijayaragavan, K., Rajiv Ganthi, R., Chidambaram, S., Anandhan, P., Manivannan, R., Vasudevan, S., 2010. Application of water quality index for groundwater quality assessment: Thirumanimuttar sub-basin, Tamilnadu. India. Environ. Monit. Assess. 171 (1-4), 595–609.

[58] Verma, O., Khosla, A., (2019), Developments in the stratigraphy of the Deccan Volcanic Province, peninsular India, Comptes rendus - Geoscience, pp.1-16

[59] Wang, X., Zhang, F., Ding, J., 2017. Evaluation of water quality based on a machine learning algorithm and water quality index for the Ebinur Lake Watershed. China. Scientific Reports. Nature. 7, 12858. https://doi.org/10.1038/s41598-017-12853-y.

[60] Wilcox, L.V., 1948. The Quality of Water for Irrigation Use. In Technical Bulletin No. 962, 1948; US Department of Agriculture, Economic Research Service: Washington, DC, USA.

[61] Wilcox, L.V., 1955. Classification and Use of IrrigationWaters; US Department of Agriculture Circular 969: Washington. DC, USA.

[62] Zhaoshi, W., Xijun, L., Kuanyi, L., 2021. Water quality assessment of rivers in Lake Chaohu Basin (China) using water quality index. Ecol. Indic. 121, https://doi.org/10.1016/j.ecolind.2020.107021